Earth and Space Science

RESEARCH ARTICLE
10.1029/2020EA001338

Special Section:
Jupiter Midway Through the Juno Mission

Thermoelastic Response of the Juno Spacecraft's Solar Array/Magnetometer Boom and Its Applicability to Improved Magnetic Field Investigation

M. Herceg[1], P. S. Jørgensen[1], J. L. Jørgensen[1], and J. E. P. Connerney[2,3]

[1]Measurement and Instrumentation, Technical University of Denmark (DTU), Lyngby, Denmark, [2]Space Research Corporation, Annapolis, MD, USA, [3]NASA Goddard Space Flight Center, Greenbelt, MD, USA

Key Points:
- We propose a model for compensation of the MAG boom flexure effect
- Modeling was based solely on the PJ1 data and the model has been applied on data well beyond that period and thermal range, up to PJ26
- The thermal modeling illustrates the need for a comprehensive systems approach in achieving high-accuracy measurements on space platforms

Correspondence to:
M. Herceg,
mher@space.dtu.dk

Citation:
Herceg, M., Jørgensen, P. S., Jørgensen, J. L., & Connerney, J. E. P. (2020). Thermoelastic response of the Juno spacecraft's solar array/magnetometer boom and its applicability to improved magnetic field investigation. *Earth and Space Science*, *7*, e2020EA001338. https://doi.org/10.1029/2020EA001338

Received 10 JUL 2020
Accepted 21 OCT 2020
Accepted article online 19 NOV 2020

Abstract Juno was inserted into a polar orbit about Jupiter on 4 July 2016. Juno's magnetic field investigation acquires vector measurements of the Jovian magnetic field using a pair of a triaxial Fluxgate Magnetometers (FGMs) colocated with four attitude-sensing star cameras on an optical bench. The optical bench is placed on a boom at the outer extremity of one of Juno's three solar arrays. The Magnetic Field investigation (MAG) uses measurements of the optical bench inertial attitude provided by the micro-Advanced Stellar Compass (μASC) to render accurate vector measurements of the planetary magnetic field. During periJoves, orientation of the MAG Optical Benches (MOB) is determined using the spacecraft (SC) attitude combined with transformations between SC and MOB coordinate frames. Substantial prelaunch effort was expended to maximize the thermomechanical stability of the Juno solar arrays and MAG boom. Nevertheless, the Juno flight experience demonstrates that the transformation between SC and MAG reference frames varies significantly in response to spacecraft thermal excursions associated with large attitude maneuvers and proximate encounters with Jupiter. This response is monitored by comparing attitudes provided by the MAG investigation's four Camera Head Units (CHUs) with those provided by the Stellar Reference Unit (SRU). These systematic variations in relative orientation are thought to be caused by the thermoelastic flexure of the Juno solar array in response to temperature excursions associated with maneuvers and heating during close passages of Jupiter. In this paper, we investigate these thermal effects and propose a model for compensation of the MAG boom flexure.

1. Introduction

As a fully autonomous star tracker, the Magnetic Field investigation (MAG)'s micro-Advanced Stellar Compass (μASC) services the Juno MAG attitude determination requirement by comparison of the observed star field with the matching star field stored in an on-board star catalog (Connerney et al., 2017). Juno's MAG boom is a 4-m extension at the outer extremity of one of Juno's three solar panel arrays (total length of 9 m). Juno is a spin-stabilized spacecraft rotating nominally at 2 rotations per minute (rpm) about an axis that is closely aligned with the spacecraft telecommunications antenna (High Gain Antenna—HGA). To optimize the attitude determination function on a spinning spacecraft, the four μASC star Camera Head Units (CHUs) are oriented on the Juno spacecraft with an angular separation of 13° between the optical and spin axes. The CHUs have an optical field of view (FOV) of 13° by 18° and scan the sky continuously in the anti-sunward direction, imaging every 0.25 s and producing attitude quaternions at the same rate (though telemetry allocations dictate their downlink cadence).

The MAG investigation was planned with several pathways to provide attitude determination for the fluxgate sensors (Connerney et al., 2017), and that flexibility proved useful when Juno's mission plan transitioned, after orbit insertion, from one with 14-day orbits to one with 53-day orbits (Bolton et al., 2017). To acquire the same number (34) of orbits provided for in the original mission plan, Juno was required to operate over a much broader range of local times than it was designed for. As a result, during most periJoves, the ASC CHUs would encounter Jupiter in the FOV for at least some portion of the time, preventing continuous attitude determination throughout the critical close passage. As a result, the MAG investigation elected a backup attitude determination strategy in which attitudes are derived from the National Aeronautics and Space Administration (NASA)'s Navigation and

Ancillary Information Facility (NAIF) (Acton, 1996; Acton et al., 2018) spacecraft attitude solution (c-kernel) using a transformation between the MAG optical bench and the spacecraft determined by comparison (when available) between the ASC CHUs and the spacecraft Stellar Reference Unit (SRU). The SRU is located on the main body of the Juno spacecraft, whereas the four μASC CHUs are located with the Fluxgate Magnetometer (FGM) sensors on the MAG boom, at the tip on the $+X$ solar wing. Since all of these sensors produce attitude quaternions continuously, we are able to intercompare the orientation of these sensors and thereby monitor the mechanical stability of the solar array structure (Wing 1) and the MAG boom.

Direct comparison of the spacecraft attitude solutions with those provided by the CHUs on the MAG boom revealed a systematic variation in the attitude of the MAG boom as Juno transited the solar system during cruise, attributed to mechanical deformation of the solar array as it cooled while moving further from the Sun (Connerney et al., 2017). Once Juno arrived in orbit around Jupiter, a similar deformation was observed during periJove passes, attributed to heating of the solar array associated with proximity to Jupiter ("Jupiter shine"). We note that the MAG boom itself proved to be remarkably stable, throughout cruise and during orbital operations, but as it is affixed to the outer end of the solar array, a distortion of the array perturbs the attitude of the MAG Boom. The solar array bends in response to the increase in temperature due to non-isotropic coefficients of thermal expansion (CTE) inherent to the design of the mechanical assemblage. The array substrate is a layer structure consisting of thin carbon-composite face sheets encasing an aluminum honeycomb core (typical of lightweight spacecraft construction). By itself, it would likely be fairly benign in its thermal response, but the sunward facing side is coated with silicon cells and cover glass with a CTE unlike that of the substrate.

The increase in temperature associated with a periJove passage is measured by multiple thermal sensors on the solar array and is just a few degrees C (about 5° or 6° for most periJoves) from a typical baseline temperature of about −130°C. However, that is sufficient to alter the boom (and hence MAG sensor) attitude by almost 0.1°. A systematic attitude error of this magnitude would directly and proportionally propagate to the pointing of the measured vector magnetic field by the FGM, contributing to a serious degradation in measurement vector accuracy, and ultimately, degradation of spherical harmonic models of Jupiter's magnetic field (e.g., Connerney, Kotsiaros, et al., 2018). Another of Juno's primary science goals, characterization of currents (e.g., Birkeland currents) in Jupiter's magnetosphere, would also be compromised, since field-aligned currents (Birkeland currents) and attitude errors both result in field components orthogonal to the vector field. The uncertainty of the magnetic field vector direction of 0.1° would, in a very strong field of Jupiter (~14 Gauss, as observed during periJove 29), create an error as large as ~2,400 nT, which is an order of magnitude larger than the field produced by Birkeland currents in Jupiter's magnetosphere (Kotsiaros et al., 2019, 2020). Of course, other less direct methods may be used to reduce, or mitigate, the effects of unwanted attitude errors, particularly if absolute vector accuracy is not required; here we adopt a physical model of the phenomenon and analytically correct the measurement platform attitude variations to recover absolute vector accuracy.

The observed thermal distortion is brief in duration (~2 hr) and the array returns to its pre-periJove attitude after thermal relaxation, but the distortion occurs at the time of highest scientific interest. Since Juno periapsis passages are just above the planet's cloud tops, the spacecraft warms with every passage, and since Jupiter has a very strong planetary magnetic field (Connerney, Kotsiaros, et al., 2018), every passage transits a strong magnetic field magnitude (~4 to ~14 G). Therefore, a significant attitude disturbance occurs upon every periJove, as well as with any spacecraft attitude maneuver that changes the spacecraft spin axis orientation relative to the Sun vector.

Identification of the thermal distortion of the solar array necessitated implementation of a time-dependent transformation between spacecraft and MAG Optical Bench (MOB), similar to the correction model applied to the Swarm satellites orbiting the Earth (Herceg et al., 2017). The objective of this study is to characterize the thermal distortion of the mechanical appendage, determine its dependence on array temperature, and offer a model whereby the MAG attitude disturbance can be predicted with confidence and removed from the data. This report also serves to bring awareness to subtle effects that may limit measurement accuracy on flight systems that do not benefit from sensors capable of monitoring mechanical stability.

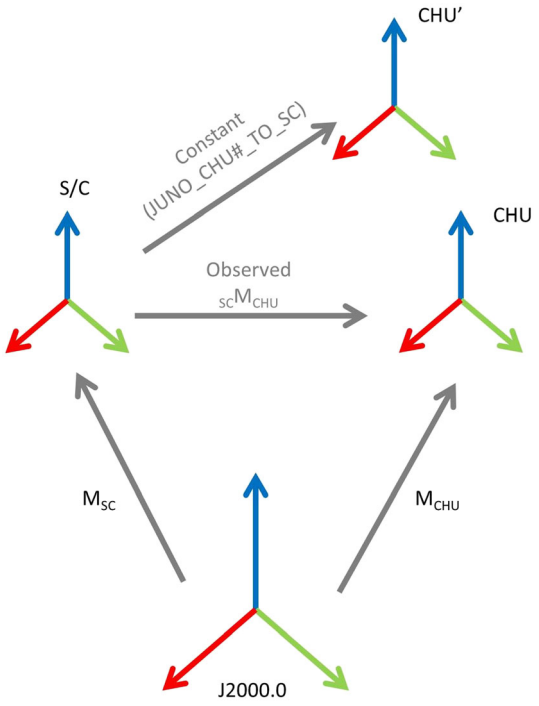

Figure 1. Coordinate frames utilized for the thermoelastic boom model and relations between them.

2. Modeling of the Thermoelastic Effects

The relevant Juno reference frames, and the transformations between them, are presented in Figure 1. M_{SC} is the transformation matrix describing the Juno spacecraft orientation in the inertial (J2000) reference frame, extracted from NASA's NAIF c-kernels, and M_{CHU} is the transformation matrix describing the orientation of a CHU in the inertial (J2000) frame, determined from μASC measurements. Juno spacecraft NAIF c-kernels are made available through merging of the attitude data derived from one or several attitude sensors combined in the most accurate solution. Retrieved quaternions are then used by Jet Propulsion Laboratory (JPL) NAIF division to construct c-kernels.

Fixed transformations between the Juno SC (defined as the center of the High Gain Antenna) and each of the four ASC CHUs (*Juno_CHU#_TO_SC*), as defined in the NAIF Frame Kernel (FK) file, are represented via sequential rotations about the spacecraft *x*, *y*, and *z* axes (see Table 1 for transformation angles and Figure 2 for frame definitions).

The transformation (see Figure 2) from the SC frame to that of the InBoard (IB) or OutBoard (OB) MAG optical bench (MOBs) was originally envisioned as a static transformation that might change from one periJove to another, perhaps in response to infrequent spacecraft propulsive maneuvers, but was assumed to remain unchanged throughout a periJove pass. The MAG boom itself proved to be remarkably stable over environmental conditions, as determined by intercomparison of the four CHUs. Each MOB contains a pair of CHUs, mounted to the MOB with kinematic mounts (as are the fluxgate sensors). The MAG boom itself is a large (~4 m long) three-dimensional structure constructed of aluminum honeycomb, carbon-composite faced sheets, with longitudinal stiffeners running the length of the structure, fully enclosed in multilayer thermal insulating blankets.

The MAG investigation anticipated the need to verify the deployment attitude of the MAG boom in flight, and periodically monitor the relationship between spacecraft attitude and MOB attitude, and as a result, a series of attitude calibration exercises were scheduled before and after major propulsive maneuvers (Connerney et al., 2017). It was learned that while propulsive maneuvers resulted in transient disturbances, the MAG boom attitude returned very close to premaneuver orientation. However, when comparing the spacecraft attitude solution during periJove passages with attitudes measured each 0.25 s by the CHUs, we observed a systematic variation quickly identified (see Figure 3) as a response of the Juno solar array to the increase in temperature due to Jupiter thermal emission. Thus, the need for a predictive model for a time-dependent transformation between spacecraft and MOB. This model helps mitigate propagation of the attitude determination error into the measured magnetic field vector and thereby increases the accuracy of the magnetic field models based upon Juno measurements.

Comparison of the CHU attitude observations and SC orientation in the CHU reference frame ($_{sc}M_{chu}$) shows a systematic variation with periJove passage, remarkably consistent from one periJove passage to the next (Figure 3) with one exception having to do with spacecraft attitude during periJove passage. Most orbits in the Juno mission plan are executed with the spacecraft spin axis, and telecom antenna, directed toward Earth for gravity science (Bolton et al., 2017). On occasion, periJoves are executed with the spin axis directed off Earth point in a manner that optimizes passage of the microwave radiometer (MWR) field of view (and that of other instruments) as it scans across the planet. These two kinds of orbits—called "GRAV" and "MWR" orbits for short—lead to different thermal responses most easily identified by the attitude of the MAG boom upon approach to periJove and the disturbance in attitude ~6 hr after periJove as the spacecraft reacquires Earth pointed attitude.

Table 1
Fixed Transformations Between the Juno SC and Each of the Four ASC CHUs, Represented via Sequential Rotations About the Spacecraft x, y, and z Axes

	Rot3 *Z*	Rot3 *Y*	Rot3 *X*
S/C–> CHU A	178.950	1.370	−167.035
S/C–> CHU B	179.125	1.150	167.035
S/C–> CHU C	−1.000	0.480	−166.480
S/C–> CHU D	−0.220	0.510	167.380

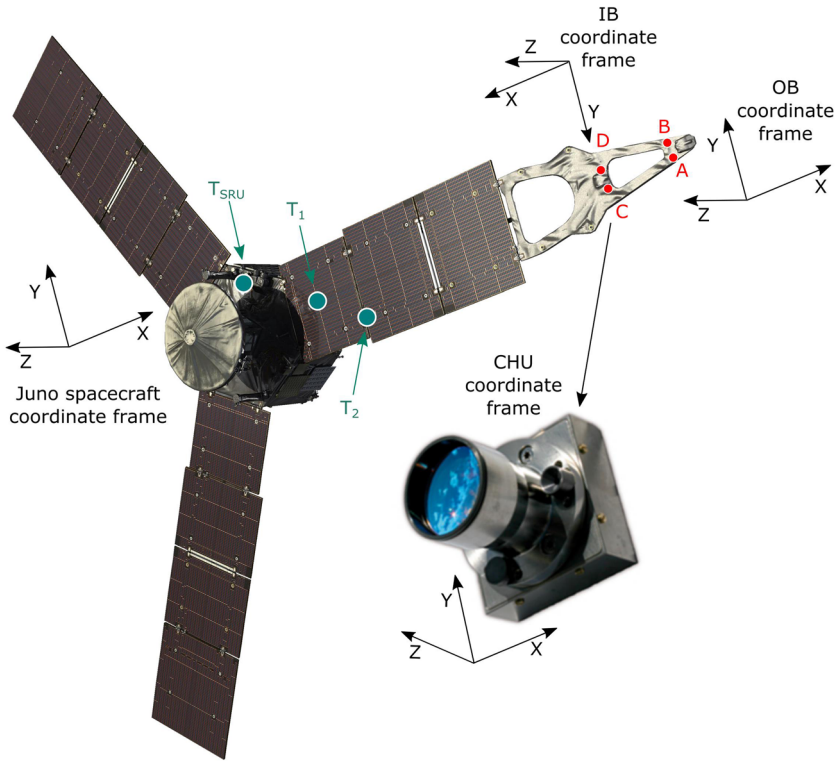

Figure 2. The Juno spacecraft, the μASC CHU and the MAG instrument coordinate frames. Turquoise circles show locations of the Wing 1 solar array thermistors (T_1 and T_2) and Stellar Reference Unit thermistors (T_{SRU}). Red circles show locations of the four μASC CHUs. Rotation about the y axis of the SC (parallel to solar panel hinge line) is where bending of the Juno Wing 1 is observed. SC + Z axis is aligned with the center of the High Gain Antenna (HGA), +X axis is in the direction of the Magnetometer Boom, and +Y axis is completing the right-hand-handed coordinate frame. Inboard and Outboard MOB frames are defined by two vectors that are the sum and the difference of the boresight directions of the two CHUs mounted on each bench: +Z axis is along the vector that is the sum of the CHUboresight directions (CHUA + CHUB for OB, CHUD + CHUC for IB), +Y axis is along the vector that is the difference of the boresight directions (CHUA − CHUB for OB, CHUD − CHUC for IB), and +X axis completes the right-handed frame.

The transformation between the SC and CHU frame is (${}_{sc}M_{chu}$) is defined as

$$ {}_{sc}M_{chu} = M_{CHU}\ \ {M_{SC}}^{T} \tag{1} $$

Comparison of the Juno CHU and SC orientation in the CHU reference frame is calculated by applying the preflight fixed transformations between the two frames:

$$ {}_{sc}M_{chu\_REL} = M_{Juno\_CHU\#\_TO\_SC} \cdot {}_{sc}{M_{chu}}^{T} \tag{2} $$

The Juno spacecraft is equipped with a multitude of thermal sensors to monitor temperatures throughout the spacecraft, including several deployed along the solar array (Wing #1) hosting the MAG boom. Two of these (T_1 and T_2 in Figure 2) have proven very useful in modeling the array response, as illustrated in Figure 4. Comparison of the temperature and attitude variation shows a clear correlation between the disturbance rotation angle about the CHU B y axis and the solar array temperature (Figures 4 and 5).

For the purpose of correcting the relative orientation between the SC and each CHU for thermal effects, a thermal compensation model was defined using valid attitude data from the very first periJove (PJ 1). A model was constructed using the orientation of each CHU with respect to the SC orientation in the camera frame combined with Juno Wing 1 solar panel temperatures T_1 and T_2. T_1 is a compact reference for Lockheed Martin's (LM) engineering telemetry channel T-0237 SA1pan1Temp, and T_2 refers to LM's

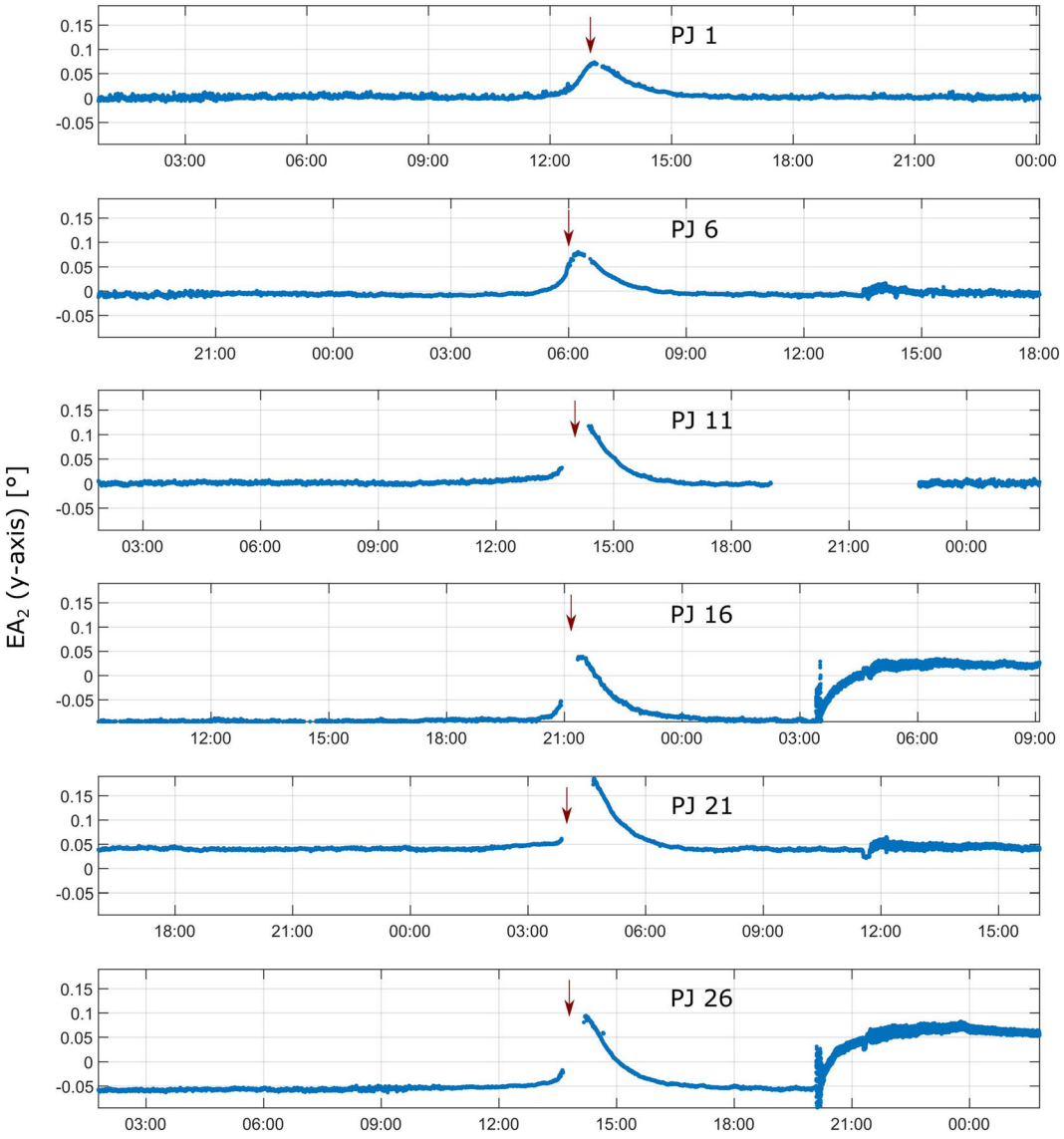

Figure 3. Comparison of the Juno CHU B and SC orientation expressed as a rotation about the spacecraft *y* axis in the CHU reference frame (for the periJoves 1, 6, 11, 16, 21, and 26). A fixed rotation about *y* axis of 1.15° (specified in the Table 1 as the fixed rotation) has been removed. PeriJoves 16 and 26 illustrate MWR orbits, in which the spacecraft approaches Jupiter off Earth point and returns to Earth pointed attitude ~6 hr post-PJ. Red arrows indicate the time of the periJove.

T-0446 SA1pan2Temp, output from Juno's Wing 1 solar panel thermistors. In addition to the solar panel temperatures, T_1 and T_2, the model uses SRU thermistors to compensate for the small quasiperiodic attitude perturbations visible on the x axis of the SC frame. These relatively minor attitude errors (in the spacecraft c-kernel attitude estimation) are caused by the slight thermal distortion of the mechanical structure supporting the SRU. This effect is visible in blue curve on the top panel of Figure 6. These perturbations correlate well with a combination of the outputs from the two thermistors associated with this subsystem; the SRU is heated by two independently controlled heaters cycling on and off in a quasiperiodic manner. We use the SRU-based temperature proxy T_{SRU} that is the mean of the SRU temperatures ($T_{\mathrm{SRU}} = (\mathrm{SRU1}_{\mathrm{Temp1}} + \mathrm{SRU2}_{\mathrm{Temp1}})/2$).

To estimate the parameters of the thermal model (rotations) based on the observed temperatures and frames differences, a Singular Value Decomposition (SVD) of the linear system of equations was used. The resulting

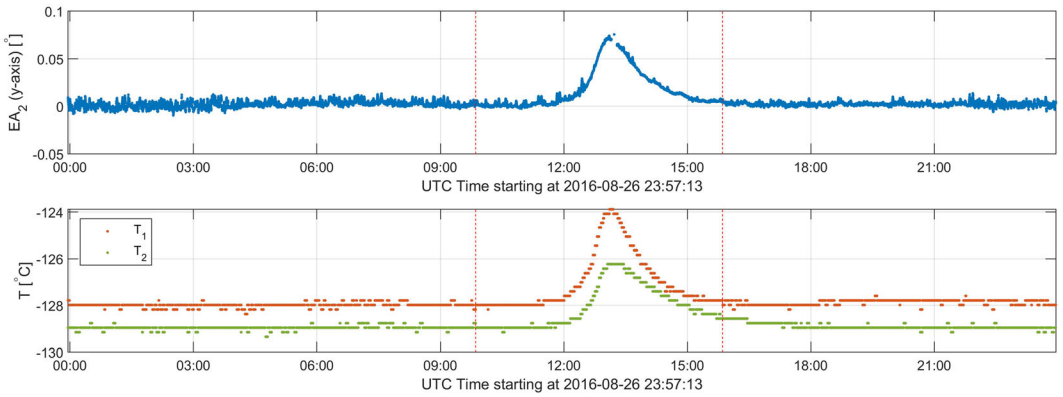

Figure 4. Juno SC rotation about the y axis in the CHU B reference frame for PJ 1 (top plot), Juno Wing 1 solar panel thermistor observations (T_1 and T_2, second plot).

thermal model describes how each transformation between CHU and SC changes due to the observed temperature of the Juno Wing 1 structure and it is defined as

$$M_{Juno\_CHU\#\_TO\_SC\_CORR} = R_1(\alpha) \cdot R_2(\beta) \cdot R_1(\gamma) \cdot M_{Juno\_CHU\#\_TO\_SC} \tag{3}$$

where each rotation is described by

$$R_1(\alpha) = \begin{bmatrix} 1 & 0 & 0 \\ 0 & \cos(\alpha) & \sin(\alpha) \\ 0 & -\sin(\alpha) & \cos(\alpha) \end{bmatrix} \tag{4}$$

$$R_2(\beta) = \begin{bmatrix} \cos(\beta) & 0 & -\sin(\beta) \\ 0 & 1 & 0 \\ \sin(\beta) & 0 & \cos(\beta) \end{bmatrix} \tag{5}$$

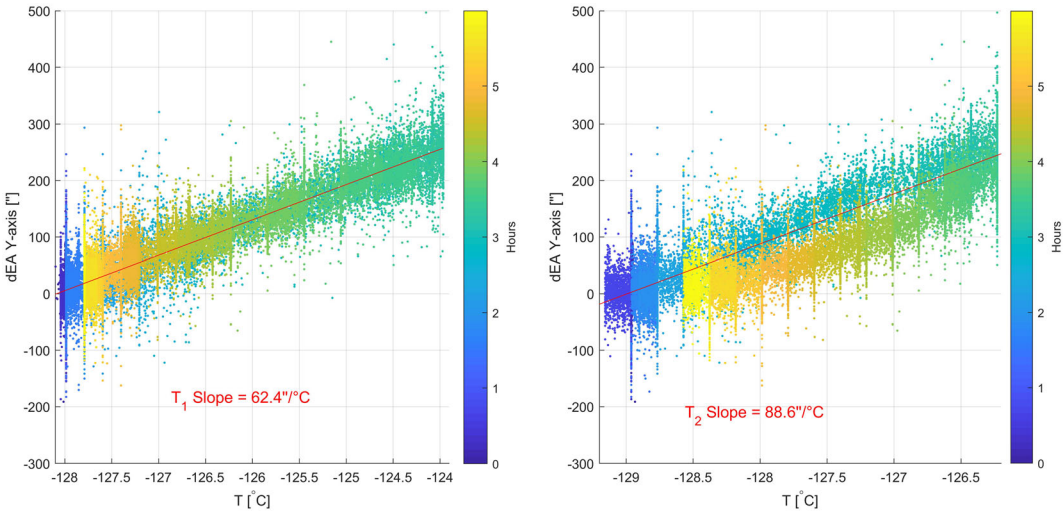

Figure 5. Correlation between the rotation about the y axis variation and Juno solar panel temperatures (T_1 and T_2). Correlation is shown for the period ±3 hr around the periJove. The relaxations of the boom bending caused by temperature variation is shown by the hysteresis of the temperature data (clearly visible on the right-hand plot).

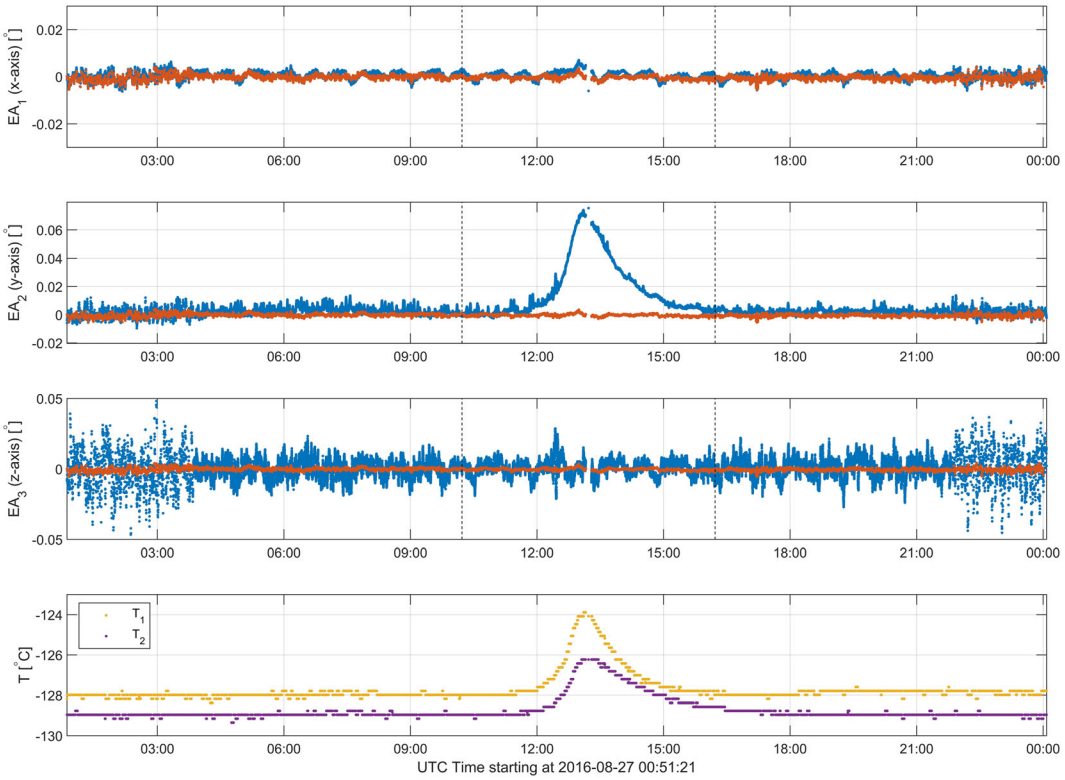

Figure 6. Relative comparison of the Juno CHU B and SC orientation in the CHU B reference frame (PJ1, 2016–240). Top three panels: Blue shows uncorrected deflection angles. Red shows deflection angles after correction and applying a 60-s moving average. Bottom panel shows the two SC solar panel temperatures.

Table 2
Thermal Model Coefficients Based on PJ 1 (2016-240) for Transformation Between Juno SC and Each of the μASC CHUs

	α	β	γ	
		CHU A		
Constant	0.0836	−2.3869	−0.3924	(°)
T_1	0.0019	−0.0140	−0.0028	(°/°C)
T_2	−0.0011	−0.0045	6.0e−05	(°/°C)
T_{SRU}	−0.0009	−8.0e−05	−0.0019	(°/°C)
		CHU B		
Constant	0.0673	−2.1642	0.4530	(°)
T_1	0.0013	−0.0131	0.0022	(°/°C)
T_2	−0.0006	−0.0036	0.0016	(°/°C)
T_{SRU}	−0.0010	−0.0009	−0.0022	(°/°C)
		CHU C		
Constant	−0.0764	2.3342	−0.5756	(°)
T_1	−0.0021	0.0138	−0.0042	(°/°C)
T_2	0.0013	0.0043	−1.0e−05	(°/°C)
T_{SRU}	0.0009	5e−05	−0.0018	(°/°C)
		CHU D		
Constant	−0.0374	2.3487	0.4798	(°)
T_1	−0.0017	0.0135	0.0039	(°/°C)
T_2	0.0013	0.0046	0.0001	(°/°C)
T_{SRU}	0.0009	0.0008	−0.0017	(°/°C)

$$R_3(\gamma) = \begin{bmatrix} \cos(\gamma) & \sin(\gamma) & 0 \\ -\sin(\gamma) & \cos(\gamma) & 0 \\ 0 & 0 & 1 \end{bmatrix} \quad (6)$$

and individual rotation angles are represented as follows:

$$\alpha = \alpha_0 + \alpha_1 T_1 + a_2 T_2 + \alpha_3 T_{SRU} \quad (7)$$

$$\beta = \beta_0 + \beta_1 T_1 + \beta_2 T_2 + \beta_3 T_{SRU} \quad (8)$$

$$\gamma = \gamma_0 + \gamma_1 T_1 + \gamma_2 T_3 + \gamma_3 T_3 \quad (9)$$

The model derived from the SVD is shown in Table 1.

Resulting thermal model coefficients derived from SVD is shown in Table 2.

As seen from the model coefficient table, the angular deviation is almost entirely a rotation about the spacecraft y axis (β), which is parallel to the solar array hinge line; this is consistent with the attitude variation observed during cruise (Connerney et al., 2017) in response to the secular cooling of the array in transit from Earth to Jupiter, during which a rotation of ~1° of rotation about spacecraft y axis was observed. It is also the rotation expected of bending due to unmatched CTE on sunward facing and dark sides of the solar array.

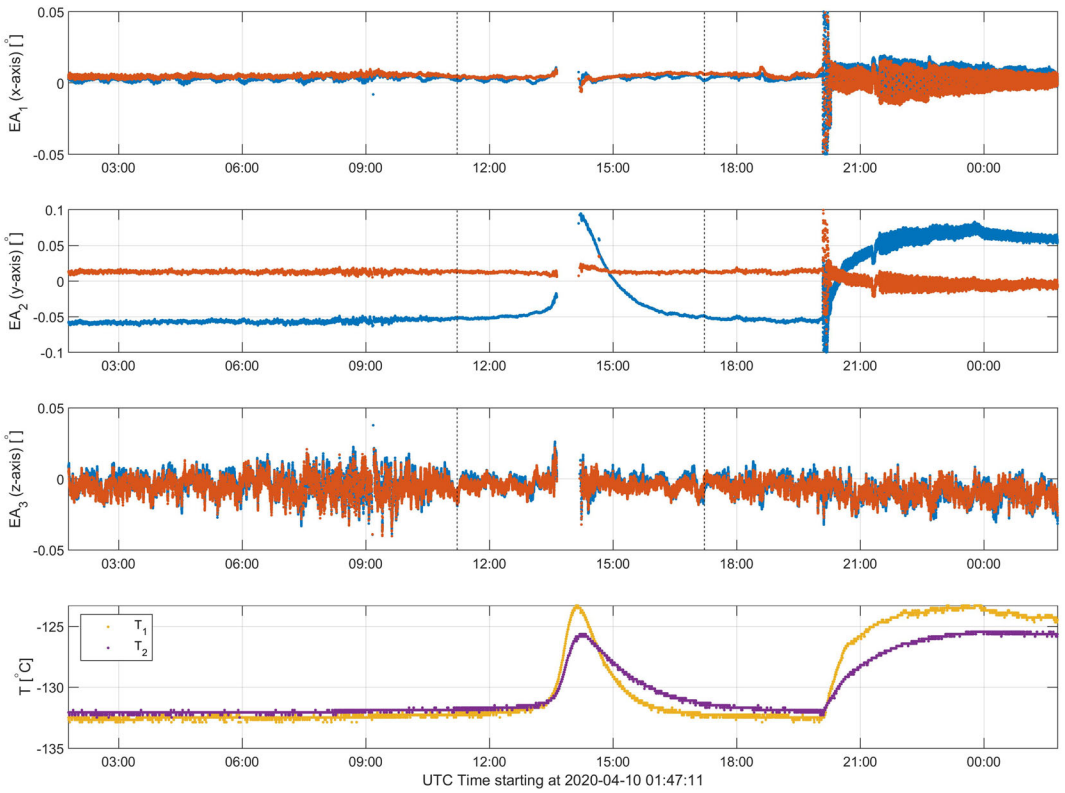

Figure 7. Relative comparison of the Juno CHU B and SC orientation in the CHU B reference frame (PJ26, 2020–101). Top three panels: Blue shows uncorrected deflection angles. Red shows deflection angles after correction and applying a 60-s moving average. Bottom panel shows the two SC solar panel temperatures.

3. Results

In Figure 6 we show a comparison of the CHU and spacecraft attitudes for periJove 1 as measured using a fixed transformation with that using a variable transformation based on the thermal model output. The corrected attitudes show significant improvements. The thermal model completely removes the variation caused by the bending of the boom (rotation about the *y* axis) and shows virtually no residual variation apart from white noise. Likewise, the quasi-periodic attitude errors appearing as rotations about the *x* and *z* axes are removed well using the SRU temperature proxy. The root-mean-square (RMS) residual attitude error of rotation about the *y* axis for periJove 1, after correction, is 8 arc-sec, compared to 72.1 arc-sec found using the uncorrected (static) transformation.

It is important to emphasize that the modeling was based only on the data from the PJ1 (2016–240). Application of the model outside of the modeling period (for the PJ3 to PJ27 data set) shows similarly good results, as seen in the example illustrated in Figure 7 for periJove 26. By applying the model to the PJ26 data, RMS of the rotation error about the *y* axis is reduced from 129.0 to 8.5 arc-sec. The uncertainty of the vector field measurement pointing direction of 129.0 arc-sec, equates to an error in the magnetic field determination of 312 nT for the maximum *B* field observed during periJove 26 (5 Gauss or 500,000 nT). The RMS improvement for periJove 26 is much larger than that for periJove 1. This is due to the orientation of the spacecraft during periapsis, and differences in the amount of heating experienced by the spacecraft during periapsis. Juno's solar array temperature (T_1) increases by around 9.5°C during periJove 26, compared to a 5°C increase experienced during periJove 1. This yields a much larger improvement in attitude error reduction, but the resulting (nominal) RMS residual error is very similar for both (around 8 arc-sec).

This is a very impressive result, considering the many years (4) separating development of the model and its application, and the range of thermal distortion accommodated (twice that used to establish the model parameters).

Figure 7 illustrates the model efficacy as applied to an MWR orbit, in which the spacecraft attitude is altered well in advance of the periJove pass (so that the spacecraft attitude perturbations are well damped). As a result, the solar array is a bit further off sun as well, and the spacecraft enters the periJove interval represented here off Earth point, and therefore somewhat cooler than normal (GRAV orbit). This effect is also well modeled and the corrected attitude is brought back to nearly 0° for the periJove. The rapid reorientation about 6 hr post-PJ is somewhat less well corrected and evidences a longer-lasting disturbance that slowly yields to the spacecraft fluid nutation dampers.

As demonstrated, the choice of the proxy temperatures and model parameters estimated with the SVD solution provide excellent compensation of the thermal disturbances. The results after applying thermal model show virtually no variation of relative orientation between SC and CHUs, apart from noise and settling effects of the Earth point precession. Note that modeling period was based solely on the PJ1 data (2016–240), and the model has been applied on data well beyond the modeling period and thermal range, up to PJ26. Using the model coefficients, a NAIF c-kernels is computed for each MOB using a thermoelastic model (Table 1) of the boom deflection as a function of temperature. These thermoelastic MOB c-kernels have been provided to NAIF for archive along with the spacecraft c-kernels (Connerney, Lawton, et al., 2018).

Performance of the proposed model for the compensation of Juno wing thermoelastic instability for periJoves 1–27 can be found in the supplementary material to this paper. Attention to mechanical stability is but one consideration in the measurement accuracy achieved on a flight platform. Juno is the first spacecraft to venture beyond Earth orbit with a magnetic field investigation suitably endowed with sensors to track attitude stability of the magnetometer boom (necessitated by the need to separate spacecraft and magnetic sensors). Juno's very accurate vector magnetic field measurements also revealed the presence of relatively small spacecraft fields generated within the conductive MAG boom structure itself as the spacecraft slowly spins (2 rpm) in the presence of a strong magnetic field (Eddy current generation). Correction for this effect was described by Kotsiaros et al. (2020) who presented a finite element model of Eddy current generation in the vicinity of the MAG sensors. This effort and the thermal modeling described here illustrate the need for a comprehensive systems approach in achieving high-accuracy measurements on space platforms.

Conflict of Interest

The authors are aware of no real or perceived conflicts of interest with respect to the results of this paper.

Data Availability Statement

All data used in this article are available in the main text and in the supporting information, as well as in the permanent archival data repository, Zenodo (Herceg et al., 2020).

Acknowledgments

We thank the project and support staff at the Jet Propulsion Laboratory (JPL), Lockheed Martin, and the Southwest Research Institute (SWRI) for the design, implementation, and operation of the Juno spacecraft. We are particularly indebted to Lockheed Martin mechanical engineer, Russ Gehring, who was responsible for the design and fabrication of the MAG boom. JPL manages the Juno mission for the principal Investigator, S. Bolton, of SWRI. This research is supported by the Juno Project under NASA grant NNM06AAa75c to SWRI, and NASA grant NNN12AA01C to JPL/Caltech. The Juno mission is part of the New Frontiers Program managed at NASA's Marshall Space Flight Center in Huntsville, Alabama.

References

Acton, C., Bachman, N., Semenov, B., & Wright, E. (2018). A look towards the future in the handling of space science mission geometry. *Planetary and Space Science*, *150*, 9–12, ISSN 0032-0633. https://doi.org/10.1016/j.pss.2017.02.013

Acton, C. H. (1996). Ancillary data services of NASA's navigation and ancillary information facility. *Planetary and Space Science*, *44*(1), 65–70.

Bolton, S. J., Lunine, J., Stevenson, D., Connerney, J. E. P., Levin, S., Owen, T. C., et al. (2017). The Juno mission. *Space Science Reviews*, *213*, 5–37. https://doi.org/10.1007/s11214-017-0429-6

Connerney, J. E. P., Benn, M., Bjarno, J. B., Denver, T., Espley, J., Jorgensen, J. L., et al. (2017). The Juno magnetic field investigation. *Space Science Reviews*, *213*, 39–138. https://doi.org/10.1007/s11214-017-0334-z

Connerney, J. E. P., Kotsiaros, S., Oliversen, R. J., Espley, J. R., Joergensen, J. L., Joergensen, P. S., et al. (2018). A new model of Jupiter's magnetic field from Juno's first nine orbits. *Geophysical Research Letters*, *45*, 2590–2596. https://doi.org/10.1002/2018GL077312

Connerney, J. E. P., Lawton, P., Kotsiaros, S., & Herceg, M. (2018). The Juno Magnetometer (MAG) standard product data record and archive volume Software Interface Specification (SIS).

Herceg, M., Jørgensen, P. S., & Jørgensen, J. L. (2017). Characterization and compensation of thermo-elastic instability of SWARM optical bench on micro Advanced Stellar Compass attitude observations. *Acta Astronautica*, *137*, 205–213. https://doi.org/10.1016/j.actaastro.2017.04.018

Herceg, M., Jørgensen, P. S., Jørgensen, J. L., Connerney, J. E. (2020) Supplementary material for Thermo-elastic response of the Juno spacecraft's solar array/magnetometer boom, Zenodo. https://doi.org/10.5281/zenodo.3936080

Kotsiaros, S., Connerney, J. E. P., Clark, G., Allegrini, F., Gladstone, G. R., Kurth, W. S., et al. (2019). Birkeland currents in Jupiter's magnetosphere observed by the polar-orbiting Juno spacecraft. *Nature Astronomy*, *3*(10), 904–909. https://doi.org/10.1038/s41550-019-0819-7

Kotsiaros, S., Connerney, J. E. P., & Martos, Y. (2020). Analysis of Eddy current generation on the Juno spacecraft in Jupiter's magnetosphere. *Earth and Space Science*, *7*, e2019EA001061. https://doi.org/10.1029/2019EA001061